# Investigating Various Force Control Techniques Effect on a Flexible Continuum Robot

Mai A. Mira [1,2], Osama A. Mousa[1,2], Ahmed H. Fahmy[1,2], Omar M. Shehata[1.2.3], and Elsayed I. Morgan[1,2]
[1]Multi-Robot Systems (MRS) Resaerch Group, Cairo, Egypt
[2]Mechatronics Department - Faculty of Engineering and Materials Science - German University in Cairo, Egypt
[3]Mechatronics Department - Faculty of Engineering - Ain Shams University Cairo, Egypt
Emails: maie12mico@gmail.com, {ahmed.hossam-aly & elsayed.morgan}@guc.edu.eg and Omar.shehata@ieee.com

***Abstract*—Continuum Robots are nature inspired manipulators capable of continuous bending along their structure to cope in environments where conventional rigid robots come short, such as constrained, or non-uniform environments. To ensure safe interaction with the environment, Force Control is needed, which ensures compliant behavior of the robot while constraining the force applied. The purpose of this paper is to first present the Continuum robot's kinematics and dynamics model using Piece-wise constant curvature method and Lagrangian Euler method for Multi-Section Continuum robot. Then, to formulate and examine four types of Force Control: Compliant Control, Impedance Control, Explicit Impedance Force Control, and Admittance Control. Simulations were conducted on MATLAB Simulink to test the Robot's model with these different controllers. The results successfully showed that the continuum robot's simulation was able to comply with the environment using the first two controllers, and also track a desired force using the other two controllers.**

***Index Terms*—soft continuum robots, kinematic modelling, dynamic modelling, force control, compliance behaviour, Impedance control, admittance control, compliance control**

## I. Introduction

Nature and engineers have evolved many walking systems, and by almost every measure, nature has demonstrated to be the better engineer. The wide range of abilities for locomotion, and manipulation in congested environments performed by invertebrate limbs such as elephant's trunks, snakes, and octopus tentacles have motivated a recent surge of research activity to recreate their capabilities through the making of Continuum (Soft) robots. CR are robots that feature a flexible continuously deformable backbone with no joints, which can bend at any point in its structure; giving it, theoretically, infinite degrees of freedom. The advantages of Soft Robots come from its superiority over rigid robots in its ability to adapt to changing environments, and performing certain tasks such as: navigation inside complex unstructured environments [1], grasping and manipulation of delicate objects, being compliant around humans [2], and providing high range of motion for medical instruments.

Manuscript received October 10, 2020; revised April 2, 2021.

## II. State of the Art

It is very challenging to model and control such a system that encompasses large degree of freedoms; thus, assumptions are made to make such a task a little easier. Piece-wise Constant Curvature method is a very widespread modeling method for CRs, as it approximates the robot as a series of constant-curvature arcs. This assumption made it possible to derive closed-form kinematics for Soft Robots by applying the methods some widely used to model rigid robots, including the (DH) method and Euler-Lagrange equations [3].

In order to comply with the environment, Force control is used. As demonstrated by [4], which explains several types of force controllers, Indirect Force control includes: Compliance, impedance, and implicit force control. While, Direct Force control includes: Hybrid Position/Force control, Admittance Control, and Explicit Force control.

In this paper, A comparative study including four of the force controllers found in the literature is performed. The Compliance Control and Impedance Control were used for compliant interaction with a dynamic environment. Additionally, explicit Impedance Force Control, and Admittance Control are compared in applying a desired force value on an obstacle in the environment.

This paper is organized as follows: First, the kinematic and dynamic model of the CR are briefly explained in sections III and IV. Then, the different Force Controllers are illustrated and explained in sections V and VI. Following them with the Simulation results in section VII and the final conclusion in VIII.

## III. Kinematics Modeling of A Multi-section Soft Continuum Robot

To simulate the system and control it, a model is needed; thus the Kinematics and Dynamics equations are derived.

### A. Multi-Section Forward Kinematics

Forward Kinematics are equations that take angle related input (Configuration Space) and outputs position related values (Task Space). Fig. 1 represents a Multi-


doi: 10.18178/ijmerr.10.5.255-260

section CR under the assumption of Piece-wise Constant curvature, where: $\theta_i$ is the angle of rotation about y-axis, $\phi_i$ is the angle of rotation about z-axis, $r_i$ is the arc's radius, and $l_i$ being the length of the section's arc.

*1) Forward Position Kinematics*: which is relating the end effector position $\vec{X}$ to the angles ϕ and θ. It has been derived in [3] by getting the Total Transformation matrix relating the base frame to the end effector frame. This is done by multiplying the Transformation matrix of each local section where $T_0^n = \prod_{i=1}^{n} T_{i-1}^{i}$ , with each local Transformation matrix being calculated by:

$$T_{i-1}^{i} = \begin{bmatrix} R_z(\phi_i) & 0 \\ 0 & 1 \end{bmatrix} \begin{bmatrix} R_y(\theta_i) & \vec{P}_i \\ 0 & 1 \end{bmatrix} \quad (1)$$

where $R_y(\theta_i)$ and $R_z(\phi_i)$ are the rotation matrices about y-axis and z-axis respectively, $\vec{P}_i = [r_i(1-\cos\theta_i), 0, r_i(\sin\theta_i)]$, and $r_i = l_i/\theta_i$

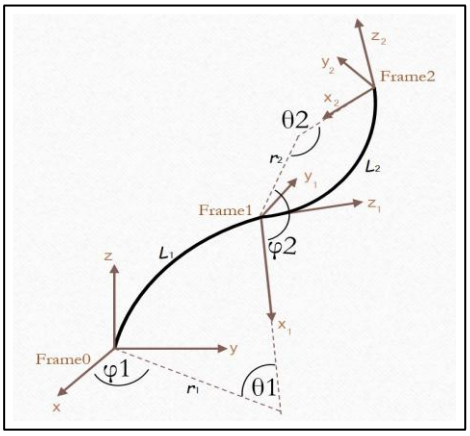


Figure 1. Double section continuum robot

By extracting the last column of the transformation matrix $T_k^i$ we can get the position vector of the i-th section end relative to the k-th frame $X_k^i$. If we are working with n sections, then

$$\vec{X} = \left[\vec{X}_0^1, \vec{X}_0^2 \dots \vec{X}_0^n\right]^T$$

*2)* Forward Velocity Kinematics: is derived as follows:

$$\dot{\vec{X}} = J(\vec{q}).\dot{\vec{q}}, with\ J = \frac{\partial \vec{X}}{\partial \vec{q}} \quad (2)$$

where $\vec{q} = [\theta_1, \phi_1, \theta_2, \phi_2 \dots \theta_n, \phi_n]$ , and $J(\vec{q})$ is the Jacobian Matrix.

*3*) *Forward Acceleration Kinematics*: is derived by differentiating equation (2), resulting in the following formula:

$$\ddot{\vec{X}} = \dot{J}(\vec{q}, \dot{\vec{q}}).\dot{\vec{q}} + J(\vec{q})\ddot{\vec{q}}\ where\ \dot{J}(\vec{q}, \dot{\vec{q}}) = \frac{\partial \dot{\vec{X}}}{\partial \vec{q}} \quad (3)$$

### B. Multi-Section Inverse Kinematics

Opposite to Forward kinematics, Inverse kinematics takes $\vec{X}$ related values as input and outputs $\vec{q}$ related values.

*1) Inverse Position Kinematics:* The same rule to get the angles $\vec{q}$ for a single section used in Paper [5], can be used for any section as long as that section's end effector's position is calculated relative to its base frame where:

$$\phi_i = \tan^{-1}\left(\frac{y_{i-1}^i}{x_{i-1}^i}\right),\ \theta_i = \cos^{-1}\left(1 - \frac{2\sqrt{{x_{i-1}^i}^2 + {y_{i-1}^i}^2}}{{x_{i-1}^i}^2 + {y_{i-1}^i}^2 + {z_{i-1}^i}^2}\right) \quad (4)$$

However, since all Position vectors $\vec{X}_0^i$ are calculated relative to the global base frame, we have to convert them to be relative to their base frame using: $\begin{bmatrix} \vec{X}_{i-1}^i \\ 1 \end{bmatrix} = \left(T_0^{i-1}\right)^{-1} \begin{bmatrix} \vec{X}_0^i \\ 1 \end{bmatrix}$

2) *Inverse Velocity & Acceleration Kinematics*: can be derived from equation 2 and 3, by solving for ~q˙ and ~q ¨respectively, resulting in:

3)

$$\dot{\vec{q}} = J^{-1}(\vec{q})\dot{\vec{X}}\ and\ \ddot{\vec{q}} = J^{-1}(\vec{q})\left(\ddot{\vec{X}} - \dot{J}(\vec{q}, \dot{\vec{q}}).\dot{\vec{q}}\right) \quad (5)$$

where $J^{-1}(\vec{q})$ is the Pseudo-Inverse of $J(\vec{q})$.

### C. Specific Mapping

All the above Kinematics is related to the independent mapping, where the actuation method doesn't matter. Moving on to the Specific Mapping, which maps between the actuator space and configuration (angle) space, the actuation is taken into consideration. In our case, we are assuming a tendon driven CR , composed of : 1 primary backbone which gives the robot its curvature, 3 secondary backbones that change length for the bending to occur, and disks to guide the tendons ; as illustrated in Fig. 2.

For section $i$, the specific Mapping equations are derived as follows: [6]

$$\vec{L}_i = \begin{bmatrix} L_{i1} \\ L_{i2} \\ L_{i3} \end{bmatrix} = \begin{bmatrix} L_i - r_d\theta_i \cos\left(\sum_{k=1}^{i} \phi_k\right) \\ L_i - r_d\theta_i \cos\left(\sum_{k=1}^{i} \phi_k + \beta\right) \\ L_i - r_d\theta_i \cos\left(\sum_{k=1}^{i} \phi_k + 2\beta\right) \end{bmatrix} \quad (6)$$

where $L_{i1}, L_{i2}$&$L_{i3}$ are the secondary backbones lengths for section $i$, $r_d$ is the distance between primary backbone and any secondary backbone, and β is the angle on the disk between two consecutive secondary backbones holes.

## IV. Dynamics Modelling Of A Multi Section Soft Continuum Robot

To describe the relation between the Angular acceleration $\ddot{\vec{q}}$, and the input Torque $\tau$, the Dynamic model must be derived. The Dynamic model is derived using the Euler Lagrangian method, which states the following:

$$\frac{d}{dt}\frac{\partial KE}{\partial \dot{q}} - \frac{\partial KE}{\partial q} + \frac{\partial PE}{\partial q} = \tau - J^T(q)F_e \quad (7)$$

where τ is the forces and moments needed to drive the system. After simplification, the dynamic equation can be written as (neglecting frictional effect):

$$M(q)\ddot{q} + C(q, \dot{q})\dot{q} + G(q) = \tau - J^T(q)F_e \quad (8)$$

where:

- $M$ is the inertia matrix
- $C$ is the matrix of centrifugal Coriolis torque
- $G$ is the gravitational matrix
- $\tau$ is the generalized torques on the system
- Fe is the external applied force at contact

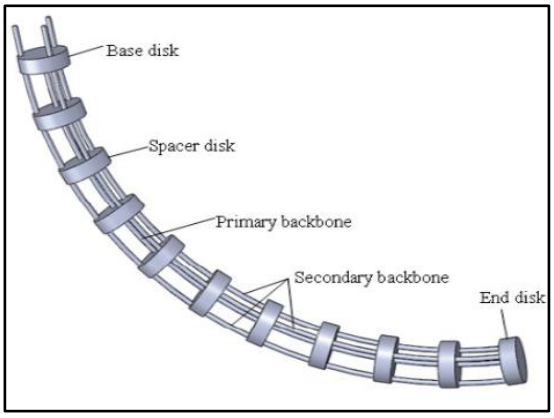


Figure 2. Design of a tendon actuated continuum manipulator [7]

Assuming our CR looks like the one in Fig. 2, then there will be three components for which Kinetic and Potential energy are derived: Primary Backbone, three Secondary Backbones, and m number of Disks per section, as extensively explained in [7] and [8].

### A. Kinetic Energy

The general Kinetic Energy equation for 3D object is:

$$KE = \frac{1}{2}mv_G^2 + \frac{1}{2}(I_{xx}\omega_x^2 + I_{yy}\omega_y^2 + I_{zz}\omega_z^2)$$

where m is the object's mass, $I_{xx}$ , $I_{yy}$ & $I_{zz}$ are the moment of inertia around x,y and z axis respectively, and $\omega_x, \omega_y$ $and$ $\omega_z$ are the angular velocities in the x, y, and z direction respectively.

However, in our soft robot, there are rotation about y (θ) and z axes (ϕ) only, therefore the term will be neglected.

To obtain the Kinetic Energy, Integration over the whole robot's length is needed. Thus new term is introduced: $s_i$ , which is section of the arc length $L_i$ upon which we will integrate. Thus, we need to get the Position Vector $\vec{X}$ as functions of $s_i$, which is done by substituting $\theta_i$ in $\vec{X}$ with $\theta_i(s_i)$, where $\theta_i(s_i) = s_i * \frac{\theta_i}{L_i}$.

The mass and moment of inertia can be defined as $dm = \rho * A * ds$ and $= \rho * I_a * ds$ . where ρ is the material's density, A is the cross sectional area and $I_a$ is the second moment of cross sectional area. Assuming that the Primary and secondary backbone's sections are composed of the same material with the same cross sectional area, and also assuming that $m_i$ disks are used in each section with a distance $h_i$ between each two consecutive disks, the Kinetic Energy can be derived using the following equation:

$$KE = \sum_{i=1}^{n} \begin{bmatrix} 4\int_0^{L_i} \frac{1}{2}\,[\,\dot{\vec{X}}_i^2(s_i)\rho A + \dot{\theta_i}^2(s_i)\rho I_{ay} \\ +\dot{\phi_i}^2(s_i)\rho I_{az}\,]\,ds_i + \frac{3m_i}{2}\,\dot{\vec{L}}_i^2 \\ +\frac{1}{2}\sum_{k=1}^{m_i}[m_{Dk}\dot{\vec{X}}_i^2(kh_i) + I_{Dk}\dot{\theta_i}^2(kh_i)] \end{bmatrix} \quad (9)$$

### B. Potential Energy

For the CR, there are two types of potential energy are considered. gravitational potential Energy caused by the force of gravity, and elastic potential energy resulting from the bending moment $\tau_{bend} = \frac{E\,I_a}{L}\theta$, where E is the module of elasticity, $I_a$ is the second moment of cross-sectional area. Accordingly, the total potential energy can be calculated as:

$$PE = \sum_{i=1}^{n} \begin{bmatrix} \frac{4EI}{2L_i}\theta_i^2 + 4\rho AL_i\vec{X}_{iCG}^T\vec{g} \\ \sum_{k=1}^{m_i} m_{DK}\vec{X}_i^T(kh_i) \end{bmatrix} \quad (10)$$

where $\vec{g}$ being the gravitational acceleration is defined in the +ve X direction, therefore it was assigned the following vector:$[9.81\ 0\ 0]^T$.

## V. Force Control For Compliant Behavior

Usually, Force control is used to minimize the interaction forces between the robot and the environment, by ensuring compliant behavior during the interaction. Two such controllers have been tested for their applicability on CRs

### A. Compliance Control

Compliance (Stiffness) Control is implemented to drive the system to behave with a desired mechanical stiffness (like a mass-spring system). Position error is related to contact forces through the stiffness of the environment and the adjusted stiffness of the robot. Then, the external force can be calculated as follows

$$F_e = k_e\,(x - x_e) \quad (11)$$

where x is the current x coordinate of the robot's end effector, which is for a double-Section CR, $x_e$ is the environment initial location, and $k_e$ is the Environment stiffness.

Usually, For Compliant control, the system is assumed to be in Steady State ($\ddot{q}$, $\dot{q}$ and $\dot{X} = 0$) since contact is assumed. Therefore, a PD control with gravity compensation is used:

$$\tau = J^T\left(k_p(x_d - x) - k_v\dot{x}\right) + G \quad (12)$$

where $k_p$ is considered the Robot's desired Stiffness. Substituting with τ in the Dynamic equation (8) would produce

$$\begin{gathered} J^T k_p(x_d - x) - J^T F_e = 0 \\ \therefore k_p(x_d - x) = F_e = k_e(x - x_e) \end{gathered} \quad (13)$$

These 2 equations are only valid in Steady State, thus Steady State Position $\vec{X}_{ss}$ and Force $F_{ess}$ can be calculated:

$$x_{ss} = \frac{k_p x_d + k_e x_e}{k_p + k_e}$$
$$\therefore F_{ess} = \frac{k_p k_e}{k_p + k_e}(x_d - x_e) = k_{eq}(x_d - x_e) \quad (14)$$

To produce a Compliant robot behavior, then $k_p$ must be way less than $k_e$, accordingly, $x_{ss} = x_e$. If a Compliant Environment is needed, then $k_p$ need to be way greater than $k_e$, then $x_{ss} = x_d$

### B. Impedance Control

Similar to Compliance Control, Impedance Control is implemented to drive the robot to behave with a desired dynamical relationship, referred to as the Target Impedance, with respect to the input contact force. where, the desired impedance is chosen as a linear second-order system so that the dynamical relationship between the force and End effector behaves like a mass spring damper system. [12] Thus:

$$F = X(m_d s^2 + d_d s + k_d) = m_d \ddot{X} + d_d \dot{X} + k_d X \quad (15)$$

To fulfill the desired Impedance performance, the robot is forced to move with the acceleration $\ddot{X}$ defined by equation (15). The corresponding configuration space acceleration $\gamma$ is calculated using equation(5) by replacing $\ddot{q}$ by $\gamma$. the robot is then driven by the torque derived using inverse dynamics control as follows:

$$\tau = M\gamma + C\dot{q} + G + J^T F_e \quad (16)$$

The equation (15) still works when robot is in free motion and accordingly, when no force is applied, it ensures position tracking, in such a case.

## VI. Force Control for Desired Force

On the other hand, other Force Controllers are used to control the applied force to track a desired value. Two such controllers are tested for their compatibility with CRs.

### A. Explicit Impedance Force Control

The same control algorithm of the Impedance Control is used, but choosing $\vec{X}_d$ to ensure a desired force value $F_{ed}$: The position is controlled to a value that ensures the occurrence of a desired Force without needing force feedback. The desired Position is chosen as follows:

$$x_d = \frac{F_e}{k_{eq}} + x_e \quad (17)$$

Thus, when substituted in equation (14), we get that $F_{ed} = F_{ess}$ and the desired Force is reached in steady state.

### B. Admittance Control

Admittance Control is a type of Force controller capable of controlling both position and force, since it has an inner motion control loop, alongside an external force control loop. Since Admittance is the inverse of Impedance, the Admittance relation is demonstrated as follows: [13]

$$X_c = \left(k_{ad} s + k_{ap} + \frac{1}{s} k_{ai}\right)(F_{ed} - F_e) \quad (18)$$

Which is exactly the configuration of a PID Controller. Accordingly, the force control law is formulated by using a PID control whose input is the error in force. Then, Xc + Xd is used as a total desired position to a position control loop that tries to reach it. To simulate the system and control it, a model is needed; thus the Kinematics and Dynamics equations are derived.

## VII. Simulations and Results

The explained Force controllers in sections V and VI have been simulated and applied using MATLAB and Simulink environment on a two section CR model, for the sake of simplicity of analysis and computation. For the two section CR simulation, the following parameters were kept constant:

| | | |
|---|---|---|
| $\theta_{i1}$ =1° | $\phi_{i1}$ =0° | $L_1$ =5$cm$ |
| $\theta_{i2}$ =2° | $\phi_{i2}$ =0° | $L_2$ =5$cm$ |

Additionally, the environment is assumed to oppose only the motion in x-axis with a stiffness $k_e = 10000$.

For this simulation, Compliance and Impedance Control have been simulated with the following common parameters:

### A. Compliant Behaviour

- Environment location:

$$x_e = \begin{cases} [0.69, 0.69, 4.86, 2.51, 3.43, 8.5]^T(\boldsymbol{cm}), t < 50\ s \\ with\ \theta_1 = 23°, and\ \phi_2 = 23° \\ [1.93, 1.93, 3.79, 4, 6.27, 4.74]^T(\boldsymbol{cm}), t \geq 50\ s \\ with\ \theta_1 = 72°, and\ \phi_2 = 72° \end{cases}$$

  with $\phi_1 = 45°$,and $\theta_2 = 40°$ in both cases.
- Desired Path is generated by choosing $\theta_2 = 45°$ and $\phi_1 = 40°$ and changing $\theta_1$ and $\phi_2$ from 0 to $90°$.

Moreover, the control gains are each assigned as:

*1) Compliance Control:*

$$k_p = 40 I_6\ , and\ k_d = 100\ I_6$$

*2) Impedance Control:*

$$k_d = 50 I_6,\ d_d = 150 I_6, m_d = 10 I_6\ ,$$

and $\dot{\vec{X}} = \ddot{\vec{X}} = 0$, where $I_6$ is a 6x6 Identity Matrix.

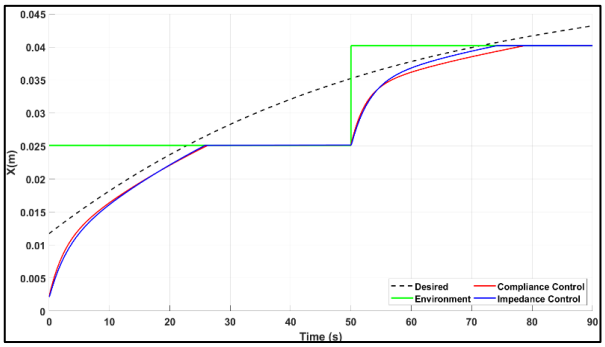


Figure 3. Two sections - X value

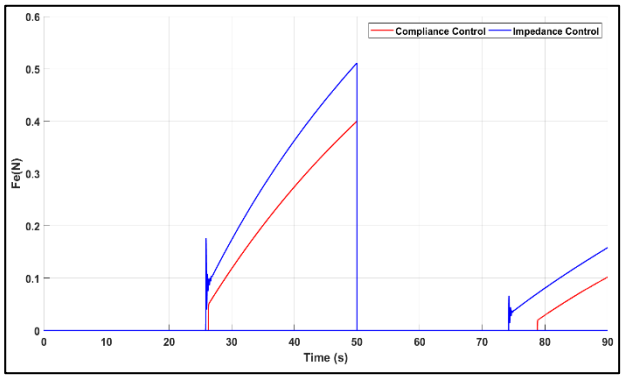


Figure 4. Two sections - force value

Figs. 3, and 4 represent the simulation results for x value and the force value respectively, for both controllers. It can be seen in figure 3 that both controllers are able to track the desired path, with small steady state error, until the robot hits the environment, to which it complies.

In comparison of both controllers, it can be observed that the Compliance control is capable of tracking the desired position with less steady state error at first, then the Impedance came to have less error in the second part. In addition, the Compliance control acts on the environment with lower force with no sudden spike, unlike the Impedance control; thus, it is concluded that Compliant control is safer and provides better compliant behaviour than Impedance Control in this application.

### *B. Force Tracking Simulation*

For this simulation, Explicit Impedance and Admittance Control have been simulated with a desired Force $F_{Des} = 0.5N$ and environment location at 0.0301 (m) in x-direction. With specific gains for each assigned as:

*1) Impedance Force Control*

$k_d = 0.2I_6$ with element (4,4) $= 100, d_d = 50\ I_6,$

$$m_d = 0.1I_6, and\ \dot{\vec{X}} = \ddot{\vec{X}} = 0$$

*2) Admittance Control*

*3)*

PID: $k_{ap} = 0.9,\ \mathrm{k_{ai}} = 0.2, k_{ad} = 0.00001,$

$\vec{X}_d = [0.0086,0,0.0490,0.401,0,0.0865],$

$k_p = I_6\ and\ k_e = 8I_6$

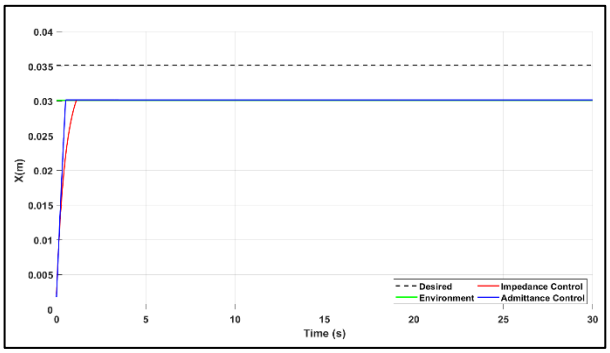


Figure 5. Two sections - X value

Figs. 5 and 6 represent the Simulation results for the x value and the force value respectively for both controllers. It is clear from the figures that Admittance Control gives a sudden force rise with 5.3 overshoot %, however the Impedance Force control has very small overshoot. Furthermore, Admittance Control has a settling time of 7.2339 sec, while Impedance Force control settled within 1.1244 sec. Thus, it can be concluded that Explicit Impedance Force Control gives better performance than Admittance Control in tracking the desired force in this application.

## VIII. CONCLUSION

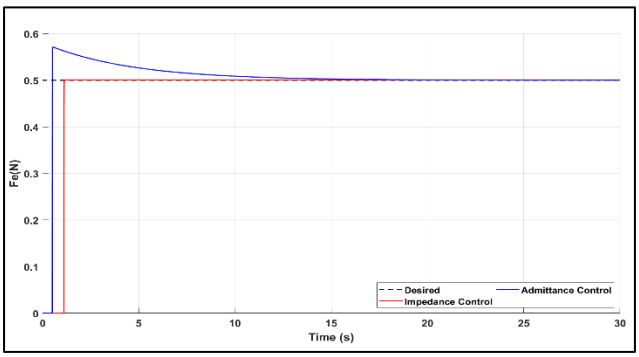


Figure 6. Two sections - force value

In this paper, CRs have been introduced, alongside their advantage over traditional rigid robot. The kinematic and dynamic model for multi-section have been derived for PCC assumption and used to simulate the system. Then, different types of Force Controllers have been illustrated and simulated on two section continuum robot model, such as Compliance control, Impedance control, Explicit Impedance Force control, and Admittance Control. Compliance and Impedance Controllers superiority over pure position control, when interacting with the environment, have been highlighted by their ability to follow a desired path, yet comply with the environment, providing a safe interaction as demonstrated in the Simulations

## CONFLICT OF INTEREST

The authors declare no conflict of interest.

## AUTHOR CONTRIBUTIONS

In this paper the research was conducted by Mai A. Mira, Osama A. Mousa and Ahmed H. Fahmy. Mai A. Mira and Ahmed H. Fahmy wrote the manuscript. The whole study was supervised by Dr. Omar M. Shehata and Prof. Elsayed I. Morgan. All authors had approved the final version.

## REFERENCES


[1] B. A. Jones and I. D. Walker, "Kinematics for multisection continuum robots," *IEEE Transactions on Robotics*, 2006.

[2] H. Lindsey and P. Kirstin, L. G. Zhan, and S. Metin, "Soft actuators for small-scale robotics," *Advanced Materials*, vol. 29, no. 13, 2016.

[3] J. W. Robert and A. J. Bryan, "Design and kinematic modeling of constant curvature CRs: A review," *The International Journal of Robotics Research*, vol. 29, no. 13, 2010.

[4] B. Aixiliano and L. Villani, *Robot Force Control*, Kluwer Academic Publishers, Boston, 1999.

[5] Arevalo, J. Carlos, and G. Elena, "Impedance control for legged robots: An insight into the concepts."

[6] N. Simaan, R. Taylor, and P. Flint, "A dexterous system for laryngeal surgery," *IEEE International Conference on Robotics and Automation*, 2004.

[7] H. Bin, W. Zhipeng, Li, Qiang, X. Hong, and S. Runjie, "An analytic method for the kinematics and dynamics of a multiple-backbone continuum robot," *International Journal of Advanced Robotic Systems*, 2013.

[8] D. Mohammad and Moosavian, S. Ali A., "Dynamics modeling of a continuum robotic arm with a contact point in planar grasp," *Journal of Robotics*, 2014.

[9] Arevalo, J. Carlos, and G. Elena, "Impedance control for legged robots: An insight into the concepts involved," *IEEE Transactions on Systems, Man, and Cybernetics, Part C (Applications and Reviews)*, 2012.

[10] Z. Ganwen and H. Ahmad, "An overview of robot force control," *Robotica*, 1997.

[11] B. Andrea, "Control, sensing, and telemanipulation of surgical continuum robots," 2013.

[12] Z. Ya-Guang, J. Bo, and L. Wei, "Leg compliance control of a hexapod robot based on improved adaptive control in different environments," *Journal of Central South University*, 2015.




**Mai A. Mira** is from Cairo, Egypt. Earned her Bachelor Degree in Mechatronics Field from the German University in Cairo (GUC), Egypt. in 2019. Main study field is Robotics and Mechatronics Engineering. She is a Teaching Assistant in the German University in Cairo Teaching different courses in the Mechatronics Department. She is an author in another published paper in ICCMA 2019, "Behavioral Assessment of Various Control Laws Formulations for Position Tracking of Multi-sectioning Modeled Continuum Robots".

**Osama A. Mousa** is from Cairo, Egypt. Earned his Bachelor Degree in Mechatronics Field from the German University in Cairo (GUC), Egypt, in 2019. Main study field is Robotics and Mechatronics Engineering.

**Ahmed H. Fahmy** is from Cairo, Egypt. Earned his Bachelor Degree in Mechatronics Field from the German University in Cairo (GUC), Egypt, in 2018. Main study field is Robotics and Mechatronics Engineering.

**Omar M. Shehata** is from Cairo, Egypt. Earned his Ph.D Degree in Mechatronics Field from Ain Shams University (ASU), Cairo, Egypt, in 2018. Main study field is Autonomous vehicles, Multi Robot Systems, Intelligent Controllers and Optimization Techniques

**ElSayed I. Morgan** is from Cairo, Egypt. Earned his Ph.D Degree in the Mechanics Field in 1972. Main study field is Robotics and Mechatronics Engineering Mechanics and Vibrations, Robotics and mechatronics engineering